Am J Cancer Res 2025;15(4):1955-1971
www.ajcr.us /ISSN:2156-6976/ajcr0163444

Original Article

Predictive value of baseline CT imaging features combined with serum biomarkers for neoadjuvant chemotherapy response in adenocarcinoma of the gastroesophageal junction

Lei Li[1*], Fei Luo[1*], Xiansheng Cao[1], Chao Zhang[1], Qi Liu[1], Shanqiang Liu[2], Libo Yu[3]

[1]Department of Gastrointestinal Surgery, Yantai Affiliated Hospital of Binzhou Medical University, Yantai 264100, Shandong, China; [2]Medical Department, Yantai Affiliated Hospital of Binzhou Medical University, Yantai 264100, Shandong, China; [3]Department of Imaging, Yantaishan Hospital, Yantai 264000, Shandong, China. [*]Equal contributors and co-first authors.

Received January 20, 2025; Accepted April 23, 2025; Epub April 25, 2025; Published April 30, 2025

Abstract: Background: Gastroesophageal junction (GEJ) adenocarcinoma, located at the esophagus-stomach junction, poses significant clinical challenges due to its complex physiological structure. Neoadjuvant chemotherapy (NAC) is standard for tumor downstaging, but response variability necessitates reliable predictive markers. This study evaluates baseline computed tomography (CT) imaging parameters and serum markers as predictors for chemotherapy response in GEJ adenocarcinoma. Methods: A retrospective study included 304 GEJ adenocarcinoma patients treated with the SOX regimen (S-1 + Oxaliplatin) between January 2020 and December 2024. Patients were categorized based on Tumor Regression Grade (TRG) into effective (TRG 0-1) and poor response (TRG 2-3) groups. Baseline CT characteristics were assessed alongside serum markers, including carcinoembryonic antigen (CEA), alpha-fetoprotein (AFP), carbohydrate antigen 19-9 (CA 19-9), and carbohydrate antigen 72-4 (CA 72-4). Multivariate logistic regression identified independent predictors, and a combined predictive model was developed and validated using an external cohort. Results: The effective treatment group showed significantly lower serum markers (CEA, AFP, CA 19-9, CA 72-4) and distinct CT parameters, including decreased maximum tumor thickness and area, and lower CT enhancement values. Extramural vascular invasion (EMVI) and tumor surface ulceration were associated with poor response. The combined predictive model demonstrated high accuracy, with an area under the curve (AUC) of 0.813 in the training set and 0.846 in the validation cohort. Conclusion: Baseline CT characteristics, when combined with serum markers, effectively predict NAC response in GEJ adenocarcinoma.

Keywords: Gastroesophageal junction adenocarcinoma, neoadjuvant chemotherapy, computed tomography, serum markers, tumor regression grade, predictive modeling

Introduction

Gastroesophageal junction (GEJ) adenocarcinoma is a malignancy located at the junction of the esophagus and stomach, an anatomical region that poses unique distinct clinical challenges due to its complex physiology and involvement with multiple organ systems [1, 2]. The incidence of GEJ adenocarcinoma has risen in recent decades, underscoring the need for effective diagnostic and therapeutic strategies [3, 4]. Neoadjuvant chemotherapy has become a standard treatment modality, offering the potential for tumor downstaging, thus increasing the likelihood of successful surgical resection and improving overall survival rates [5-7]. However, the heterogeneity of treatment response remains a significant obstacle, complicating efforts to determine optimal therapeutic strategies and highlighting the necessity for predictive markers of chemotherapy response.

Current predictive models for treatment response in GEJ adenocarcinoma primarily rely on clinical and histopathological criteria [8, 9]. These methods, however, are often limited by invasiveness, high cost, and occasional lack of specificity. Consequently, there has been grow-

https://doi.org/10.62347/XLSV6197

ing interest in non-invasive imaging and serum biomarkers as more reliable predictors of chemotherapy response, enabling the development of personalized treatment regimens.

Computed tomography (CT) imaging is routinely used in the staging and restaging of GEJ adenocarcinoma due to its wide availability and ability to provide detailed visualization of tumor morphology and regional lymph node involvement [10, 11]. Recent advancements in imaging technologies and analytic methodologies have facilitated more sophisticated assessments of tumor characteristics, including volumetric analyses, enhancement patterns, and texture analysis, which may correlate with treatment responses [12, 13]. For instance, studies have shown that parameters such as tumor attenuation coefficients and volumetric changes can provide valuable prognostic information about tumor biology and the likelihood of a favorable chemotherapy response [14].

Meanwhile, the assessment of serum markers has garnered attention due to its non-invasive nature and potential to reflect underlying tumor pathophysiology. Specific serum markers, such as carcinoembryonic antigen (CEA), cancer antigen 19-9 (CA 19-9), and newer markers, have been evaluated for their prognostic value across various cancers, including GEJ adenocarcinoma [15]. These markers may offer insights into tumor burden, biological aggressiveness, and mechanisms of chemotherapy sensitivity or resistance.

The integration of CT imaging characteristics with serum biomarker profiles offers a promising paradigm in oncology, potentially providing a comprehensive assessment that overcomes the limitations of each modality when used separately. Despite the promise of combined imaging and serum marker analyses, there is a paucity of studies investigating their predictive value specifically in GEJ adenocarcinoma. This study aims to explore the predictive value of baseline CT imaging characteristics in combination with serum markers for predicting response to neoadjuvant chemotherapy in patients with GEJ adenocarcinoma.

Materials and methods

Case selection

This retrospective case-control study included patients with GEJ adenocarcinoma who received neoadjuvant chemotherapy using the SOX regimen (S-1 [tegafur] + oxaliplatin) at Yantai Mountain Hospital from January 2020 to December 2024.

Inclusion Criteria: (1) Histologically confirmed adenocarcinoma of the GEJ through endoscopic pathological examination prior to treatment [16]; (2) Age between 18 and 85 years; (3) Preoperative tumor staging of cT3 to cT4, N0 to N3, M0 (based on combined CT evaluation); (4) Underwent radical gastrectomy following standardized neoadjuvant chemotherapy with the SOX regimen (S-1 + Oxaliplatin) preoperatively; (5) No additional treatments before the commencement of neoadjuvant chemotherapy; (6) Availability of complete clinical data, including complete hematological indices, imaging data, and postoperative pathology reports.

Exclusion Criteria: (1) Presence of concurrent malignancies; (2) Evidence of distant metastasis before neoadjuvant chemotherapy or surgery, leading to conversion or palliative treatment; (3) Non-compliance with the neoadjuvant chemotherapy protocol; (4) Tumor thickness in the gastric wall less than 1 cm, or the tumor not clearly visualized on imaging; (5) Poor quality of CT images precluding accurate measurement of relevant indicators; (6) Incomplete imaging, clinical, or pathological data; (7) Mental or cognitive impairments that prevented understanding or compliance with study requirements; (8) Pregnant or breastfeeding women; (9) History of allergy or intolerance to any component of the SOX regimen; (10) Severe cardiovascular disease (e.g., recent myocardial infarction, unstable angina), liver or kidney dysfunction, or other significant comorbidities affecting life expectancy.

Patients were categorized into two groups based on their response to chemotherapy, in accordance with the Tumor Regression Grade (TRG) criteria established by the National Comprehensive Cancer Network (NCCN) standards [17]. The effective treatment group included 106 patients, while the poor response group comprised 198 patients. Additionally, 208 patients who met the same inclusion, exclusion, and grouping criteria were incorporated into the test set for external validation. These patients were similarly categorized into an effective treatment group (n=93) and a poor response group (n=115). A flowchart illustrat-

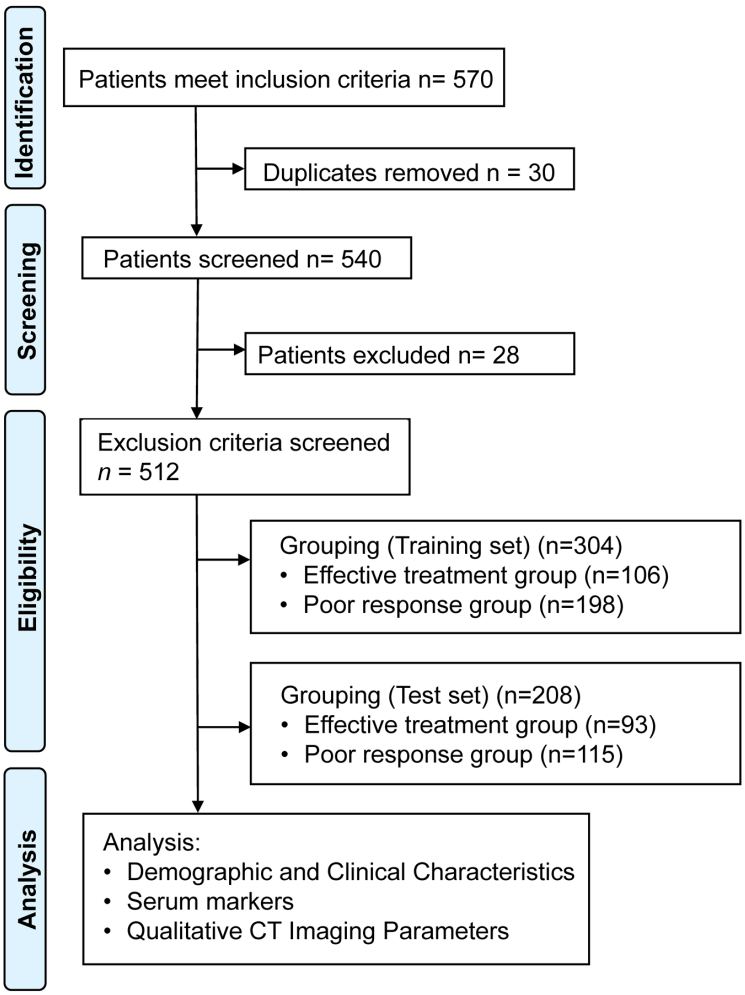

Figure 1. Patient selection flowchart. Note: CT: Computed Tomography.

ing patient selection is shown in **Figure 1**. This study was approved by the Ethics Review Committee of Yantai Mountain Hospital and strictly adhered to the ethical principles outlined in the Declaration of Helsinki. Given the retrospective nature of the study, the requirement for patient informed consent was waived.

Intervening methods

All patients received neoadjuvant chemotherapy with the SOX regimen (S-1 [Tegafur] + oxaliplatin), consisting of oral S-1 at 40 mg/m^2 twice daily for 14 days, followed by a 7-day rest, and intravenous oxaliplatin at 130 mg/m^2 on day 1 of each 3-week cycle. Patients underwent 2 to 3 cycles of chemotherapy before radical gastrectomy, which involved total or subtotal gastrectomy with lymph node dissection. Supportive care included antiemetics and periodic monitoring for side effects. Postoperative management involved monitoring for complications and recommending adjuvant chemotherapy for high-risk patients.

Data collection

(1) Baseline Data Collection: Baseline demographic information was collected from patient electronic medical records for all enrolled patients.

(2) Blood Testing: A 5 ml fasting venous blood sample (at least 8 hours) was collected from each patient. The sample was then centrifuged at 3,000 rpm for 5 minutes to obtain the supernatant. Enzyme-linked immunosorbent assay (ELISA) was used to measure levels of CEA, Alpha-Fetoprotein (AFP), Carbohydrate Antigen 19-9 (CA19-9), and Carbohydrate Antigen 72-4 (CA72-4). Specific reagent kits included CEA (ab264604, Abcam, USA), AFP (ab108838, Abcam, USA), CA19-9 (ab198-496, Abcam, USA), and CA72-4 (LZ-E028588, Shanghai Lianzu Biotechnology Co., Ltd., China). All procedures were conducted in accordance with the instructions provided in the reagent kit manuals.

(3) CT Examination Methods: Contrast-enhanced CT scans were conducted on patients before and after neoadjuvant chemotherapy. Patients were instructed to fast for 8 hours prior to the procedure. In the absence of contraindications, 10 mg anisodamine (654-2) was administered intravenously 15-20 minutes prior to the scan to reduce gastrointestinal motility. Furthermore, patients consumed 3 to 6 grams of effervescent powder orally just before the scan to ensure stomach distension. The scans were performed using a Siemens 64-slice CT scanner. The scan field spanned from the diaphragm to the bifurcation of the

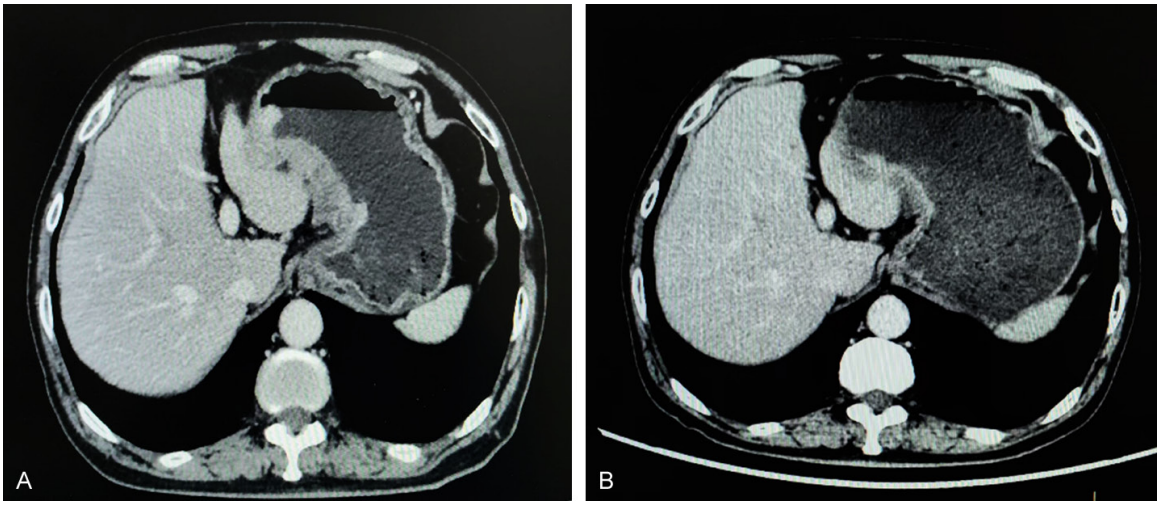

Figure 2. A patient with esophagogastric junction adenocarcinoma. A. The scan shows uneven thickening of the gastric wall; B. The post-neoadjuvant chemotherapy CT scan for the same patient, demonstrating a significant reduction in gastric wall thickening. Note: CT: Computed Tomography.

abdominal aorta. The tube voltage was adjusted automatically within the range of 120 to 140 kV, and the tube current was modulated accordingly. Imaging was conducted using a slice thickness of 1.5 mm with a pitch of 0.9. For enhanced imaging, 100 mL of a non-ionic iodine contrast agent was injected intravenously via a high-pressure injector at a rate of 3 mL/second. Arterial phase and venous phase images were acquired 40 and 70 seconds post-injection, respectively. The images were reconstructed in axial, coronal, and sagittal planes using a 0.625 mm slice thickness and a reconstruction thickness of 5 mm. Subsequently, the images were then transferred to the PACS workstation for evaluation by two radiologists.

Outcome measurement

TRG criteria: Grade 0 (complete regression): no residual tumor cells detectable under microscopy; Grade 1 (moderate regression): only isolated or small clusters of residual cancer cells present; Grade 2 (minimal regression): residual tumor present, but less extensive than the fibrotic stroma; Grade 3 (no regression): extensive residual tumor with minimal or no necrosis of tumor cells. TRG grades 0 to 1 were classified as effective treatment, whereas TRG grades 2 to 3 were considered indicative of a poor response. These criteria provide a structured approach for evaluating the effectiveness of neoadjuvant chemotherapy and categorizing patients accordingly.

CT evaluation criteria: CT Imaging Evaluation Criteria [18]: Variations in tumor enhancement patterns were assessed by comparing tumor characteristics before and after treatment (**Figure 2**). A change was recorded if a tumor that initially exhibited layered enhancement lost this feature after treatment or if a uniformly enhanced tumor developed layered enhancement post-treatment. Positive extramural vascular invasion (EMVI) was assessed according to established guidelines in the literature. For precise measurement of the tumor's maximum area and thickness, the largest cross-section on axial images was selected, ensuring no interference from adjacent gastric wall structures. Consistent layers were measured before and after treatment to minimize potential errors from varying scan angles. The maximum tumor thickness was defined as the diameter at its thickest point, and the maximum area refers to the total coverage within that section. Furthermore, the tumor enhancement value, quantified in Hounsfield Units (HU), was measured during the venous phase at the tumor's maximum area, indicating changes in tissue density. These criteria provide a systematic approach for evaluating tumor alterations before and after neoadjuvant chemotherapy, offering essential insights into the prediction of treatment efficacy.

Model development

To predict poor response to neoadjuvant chemotherapy in gastroesophageal junction ade-

nocarcinoma (GEJ) adenocarcinoma, we developed a comprehensive predictive model using the random forest algorithm. Bootstrap samples were drawn from the original dataset to construct each decision tree, with different features selected for splitting at each node. The variables included in the model included: TRG (ranging from 0 to 3), CEA, AFP, CA19-9, CA72-4, maximum tumor thickness, and maximum tumor area. These variables were chosen based on their predictive value and ranked according to their importance. Final predictions were made using majority voting (for classification problems) or averaging (for regression problems). Model performance was assessed using out-of-bag (OOB) error rate plots and variable importance plots.

Statistical method

Measurement data were presented as either mean ± standard deviation or median (interquartile range), depending on the distribution of the data. Unpaired t-tests were used to compare continuous variables between the two groups. Multivariate logistic regression analyses were conducted to determine the odds ratio (OR) and 95% confidence interval (CI) for each parameter, treating the parameters as continuous variables. Categorical data were expressed as frequencies and percentages. Chi-square tests were employed to compare proportions across groups for nominal categorical variables, such as tumor ulceration status (present vs. absent) and extramural venous invasion (EMVI) presence (yes vs. no). For ordinal categorical variables, such as education level (years) and CT enhancement values (categorized into low, medium, and high), Cochran-Armitage trend tests were used to assess trends across ordered categories. Spearman's rank correlation coefficient was used to assess correlations between variables. A *P* value of less than 0.05 was considered statistically significant. All statistical analyses were performed using SPSS software version 19 (SPSS Inc., Chicago, IL, USA) and the R software package version 3.0.2 (Free Software Foundation, Inc., Boston, MA, USA).

Results

General information (training set)

There were no statistically significant differences between the effective treatment group (n=106) and the poor response group (n=198) in most baseline characteristics, including age, BMI, education level, gender distribution, employment status, residential status, marital status, smoking history, drinking history, and incidence of hypertension, diabetes mellitus, cardiovascular disease, Lauren classification, ECOG performance status, weight loss at baseline and during neoadjuvant chemotherapy (NAC), and dysphagia score (P>0.05) (**Table 1**). Although not statistically significant, differences were noted in T stage distribution, with a higher proportion of T3 tumors in the effective treatment group compared to the poor response group, as well as variations in N stage distribution, which may reflect differences in nodal involvement (P>0.05). The distribution of Siewert types also varied, with Type II being more prevalent in both groups (P>0.05). Overall, baseline patient characteristics showed limited utility as predictors for chemotherapy response in this cohort.

Baseline serum markers (training set)

The effective treatment group exhibited significantly lower levels of CEA, with a mean of 4.56 ± 2.12 ng/mL, compared to 5.42 ± 2.54 ng/mL in the poor response group (P=0.002) (**Figure 3A**). Similarly, AFP levels were lower in the effective treatment group at 7.29 ± 3.67 ng/mL versus 8.54 ± 3.12 ng/mL in the poor response group (P=0.002) (**Figure 3B**). There was also a significant difference in CA19-9 levels, with the effective treatment group showing 28.45 ± 10.76 U/mL compared to 32.37 ± 11.12 U/mL in the poor response group (P=0.003) (**Figure 3C**). Furthermore, levels of CA72-4 were lower in the effective treatment group (6.78 ± 2.45 U/mL) than in the poor response group (7.73 ± 2.87 U/mL; P=0.004) (**Figure 3D**). Each of these serum markers demonstrated significant predictive value for distinguishing between effective and poor response to neoadjuvant chemotherapy in this cohort.

Qualitative CT imaging parameters at baseline (training set)

Tumor surface ulceration was significantly less frequent in the effective treatment group, occurring in 22.64% of patients compared to 39.39% in the poor response group (P=0.003) (**Table 2**). Similarly, EMVI was significantly less common in the effective treatment group, with

Table 1. Comparison of demographic and baseline characteristics between the two groups in the training set

Parameters	Effective Treatment Group (n=106)	Poor Response Group (n=198)	t/χ^2	P
Age (years)	62.47 ± 8.83	63.21 ± 8.32	0.725	0.469
BMI (kg/m^2)	24.12 ± 2.64	23.98 ± 2.52	0.435	0.664
Education Level (years)	12.45 ± 3.21	12.78 ± 3.15	0.870	0.385
Gender [n (%)]			0.003	0.954
Male	73 (68.87%)	137 (69.20%)		
Female	33 (31.13%)	61 (30.80%)		
Employment, work for pay [n (%)]	67 (63.21%)	124 (62.63%)	0.01	0.920
Residential Status [n (%)]			0.029	0.864
Rural	29 (27.36%)	56 (28.28%)		
Urban	77 (72.64%)	142 (71.72%)		
Marital Status [n (%)]			0.083	0.959
Married	89 (83.96%)	166 (83.84%)		
Single	11 (10.38%)	22 (11.11%)		
Divorced	6 (5.66%)	10 (5.05%)		
Smoking history [n (%)]	34 (32.08%)	67 (33.84%)	0.097	0.756
Drinking history [n (%)]	27 (25.47%)	52 (26.26%)	0.022	0.881
Hypertension [n (%)]	38 (35.85%)	72 (36.36%)	0.008	0.929
Diabetes Mellitus [n (%)]	15 (14.15%)	32 (16.16%)	0.214	0.644
Cardiovascular Disease [n (%)]	12 (11.32%)	24 (12.12%)	0.042	0.837
T Stage [n (%)]			1.769	0.184
T3	62 (58.49%)	100 (50.51%)		
T4	44 (41.51%)	98 (49.49%)		
N Stage [n (%)]			7.245	0.064
N0	19 (17.92%)	17 (8.60%)		
N1	28 (26.42%)	48 (24.24%)		
N2	31 (29.25%)	78 (39.39%)		
N3	28 (26.42%)	55 (27.78%)		
Siewert Type [n (%)]			4.244	0.120
Siewert I	2 (1.89%)	2 (1.01%)		
Siewert II	85 (80.19%)	140 (70.71%)		
Siewert III	19 (17.92%)	56 (28.28%)		
Lauren classification			0.268	0.875
Intestinal	85 (80.19%)	158 (79.80%)		
Diffuse	16 (15.09%)	28 (14.14%)		
Mixed	5 (4.72%)	12 (6.06%)		
ECOG PS			0.637	0.425
0	27 (25.47%)	59 (29.80%)		
≥ 1	79 (74.53%)	139 (70.20%)		
Weight loss at baseline (kg)	6.51 ± 1.26	6.72 ± 1.38	1.303	0.194
Weight loss during NAC (kg)	1.25 ± 0.58	1.37 ± 0.67	1.558	0.120
Dysphagia score	1.15 ± 0.34	1.21 ± 0.38	1.360	0.175

Note: BMI: body mass index; ECOG PS: *Eastern Cooperative Oncology Group Performance Status;* NAC: Neoadjuvant chemotherapy; T Stage: Tumor Stage; N Stage: Node Stage.

a rate of 9.43% compared to 21.21% in the poor response group (P=0.009). Other imaging characteristics, such as layered enhancement of the tumor (42.45% vs. 41.41%; P=0.861),

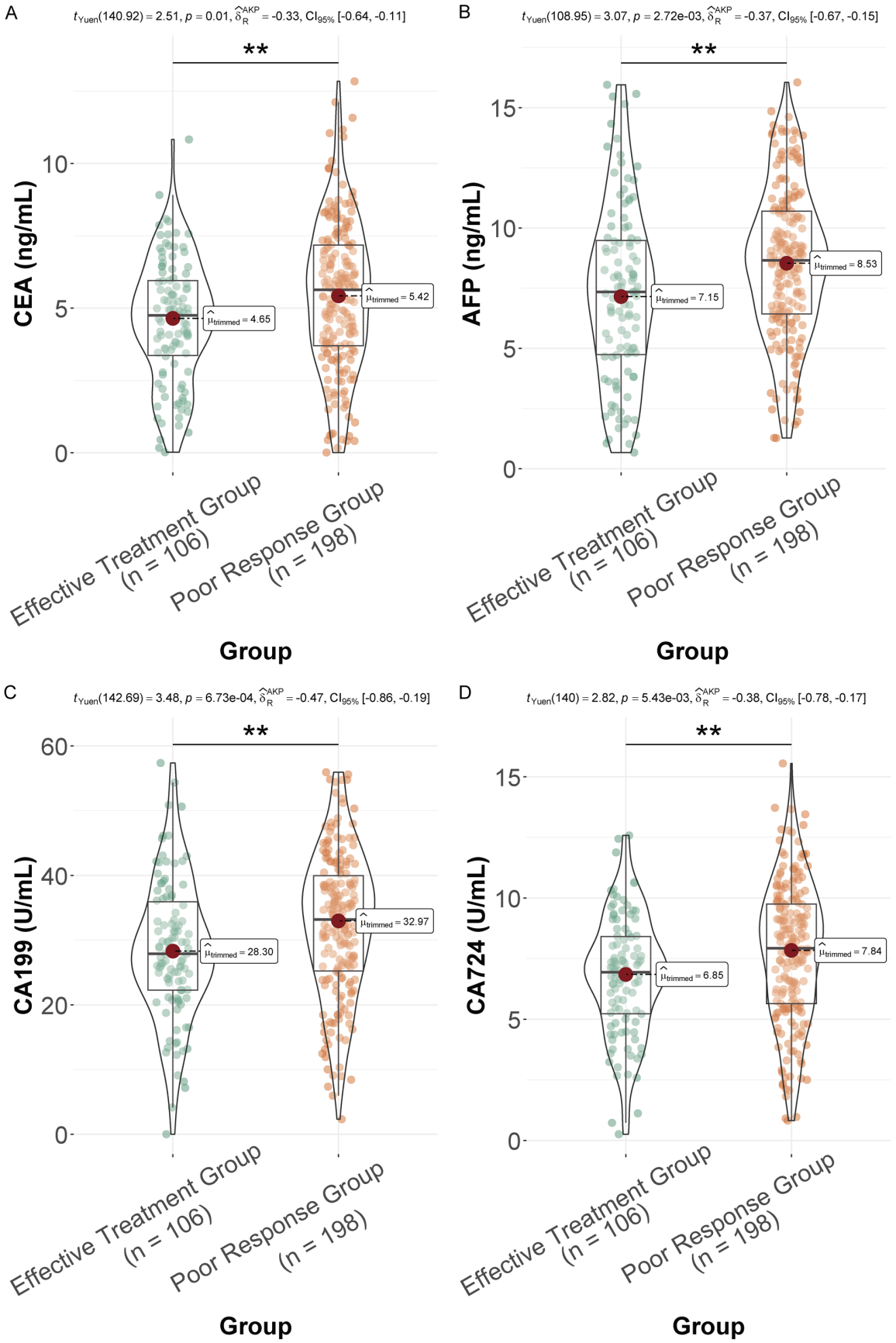
A
$t_{Yuen}(140.92) = 2.51, p = 0.01, \hat{\delta}_R^{AKP} = -0.33, CI_{95\%}$ [-0.64, -0.11]
**
CEA (ng/mL)
0
5
10
$\hat{\mu}_{trimmed} = 4.65$
$\hat{\mu}_{trimmed} = 5.42$
Effective Treatment Group (n = 106)
Poor Response Group (n = 198)
Group
B
$t_{Yuen}(108.95) = 3.07, p = 2.72e-03, \hat{\delta}_R^{AKP} = -0.37, CI_{95\%}$ [-0.67, -0.15]
**
AFP (ng/mL)
0
5
10
15
$\hat{\mu}_{trimmed} = 7.15$
$\hat{\mu}_{trimmed} = 8.53$
Effective Treatment Group (n = 106)
Poor Response Group (n = 198)
Group
C
$t_{Yuen}(142.69) = 3.48, p = 6.73e-04, \hat{\delta}_R^{AKP} = -0.47, CI_{95\%}$ [-0.86, -0.19]
**
CA199 (U/mL)
0
20
40
60
$\hat{\mu}_{trimmed} = 28.30$
$\hat{\mu}_{trimmed} = 32.97$
Effective Treatment Group (n = 106)
Poor Response Group (n = 198)
Group
D
$t_{Yuen}(140) = 2.82, p = 5.43e-03, \hat{\delta}_R^{AKP} = -0.38, CI_{95\%}$ [-0.78, -0.17]
**
CA724 (U/mL)
0
5
10
15
$\hat{\mu}_{trimmed} = 6.85$
$\hat{\mu}_{trimmed} = 7.84$
Effective Treatment Group (n = 106)
Poor Response Group (n = 198)
Group

Figure 3. Comparison of Baseline Serum Markers Between the Two Groups in the Training Set. (A) CEA; (B) AFP; (C) CA199; (D) CA724. **P<0.01. Note: CEA: Carcinoembryonic Antigen; AFP: Alpha-Fetoprotein; CA199: Carbohydrate Antigen 19-9; CA724: Carbohydrate Antigen 72-4.

Table 2. Comparison of qualitative CT imaging parameters at baseline between the two groups in the training set

Parameters	Effective Treatment Group (n=106)	Poor Response Group (n=198)	χ^2	P
Tumor Surface Ulceration	24 (22.64%)	78 (39.39%)	8.691	0.003
Layered Enhancement of Tumor	45 (42.45%)	82 (41.41%)	0.031	0.861
Vascular Invasion	17 (16.04%)	49 (24.75%)	3.081	0.079
Peritoneal Invasion	8 (7.55%)	28 (14.14%)	2.876	0.090
EMVI Positive	10 (9.43%)	42 (21.21%)	6.755	0.009

Note: EMVI, Extramural Vascular Invasion.

vascular invasion (16.04% vs. 24.75%; P= 0.079), and peritoneal invasion (7.55% vs. 14.14%; P=0.090), did not display statistically significant differences between the groups. These findings suggest that certain qualitative CT imaging parameters, particularly tumor surface ulceration and EMVI, may possess predictive value in assessing response to neoadjuvant chemotherapy in GEJ adenocarcinoma.

Quantitative CT imaging parameters at baseline (training set)

Patients in the effective treatment group exhibited significantly lower maximum tumor thickness, averaging 1.37 ± 0.38 cm, compared to 1.58 ± 0.38 cm in the poor response group (P<0.001) (**Figure 4A**). Similarly, the maximum tumor area was smaller in the effective treatment group, with a mean of 8.47 ± 2.64 cm^2 compared to 9.62 ± 2.87 cm^2 in the poor response group (P<0.001) (**Figure 4B**). Additionally, the tumor CT enhancement value was significantly lower in the effective treatment group, at 55.76 ± 6.83 HU versus 59.41 ± 6.49 HU in the poor response group (P<0.001) (**Figure 4C**). These quantitative CT characteristics demonstrate substantial predictive value for distinguishing between patients who respond effectively to neoadjuvant chemotherapy and those who do not.

Univariate correlation analysis (training set)

Univariate correlation analysis identified several factors significantly associated with a poor response to neoadjuvant chemotherapy in GEJ adenocarcinoma (**Table 3**). Among serum markers, CEA showed a positive correlation with poor response (ρ=0.163, P=0.004), as did AFP (ρ=0.178, P=0.002), CA19-9 (ρ=0.181, P=0.002), and CA72-4 (ρ=0.171, P=0.003). Qualitative CT imaging parameters, such as tumor surface ulceration also correlated positively (ρ=0.169, P=0.003), along with EMVI positivity (ρ=0.149, P=0.009). Quantitative CT imaging parameters exhibited stronger correlations, with maximum tumor thickness (ρ= 0.242, P<0.001), maximum tumor area (ρ= 0.203, P<0.001), and tumor CT enhancement value (ρ=0.249, P<0.001) all significantly correlated with poor treatment response. These findings emphasize the predictive value of both serum markers and CT imaging characteristics, with quantitative CT parameters displaying particularly strong associations.

Multivariate logistic regression analysis (training set)

The multivariate logistic regression analysis identified several independent risk factors for poor response to neoadjuvant chemotherapy in GEJ adenocarcinoma (**Table 4**). Among the serum markers, elevated levels of CEA were associated with an increased risk of poor response (OR, 1.141; 95% CI, 1.011-1.288; P=0.033), as were higher levels of AFP (OR, 1.121; 95% CI, 1.029-1.221; P=0.009), CA19-9 (OR, 1.041; 95% CI, 1.014-1.069; P=0.003), and CA72-4 (OR, 1.180; 95% CI, 1.064-1.308; P=0.002). CT imaging characteristics also played a crucial role, with tumor surface ulceration significantly increasing the odds of poor response (OR, 2.443; 95% CI, 1.288-4.633; P=0.006), as well as EMVI (OR, 2.704; 95% CI, 1.158-6.314; P=0.022). Quantitative imaging

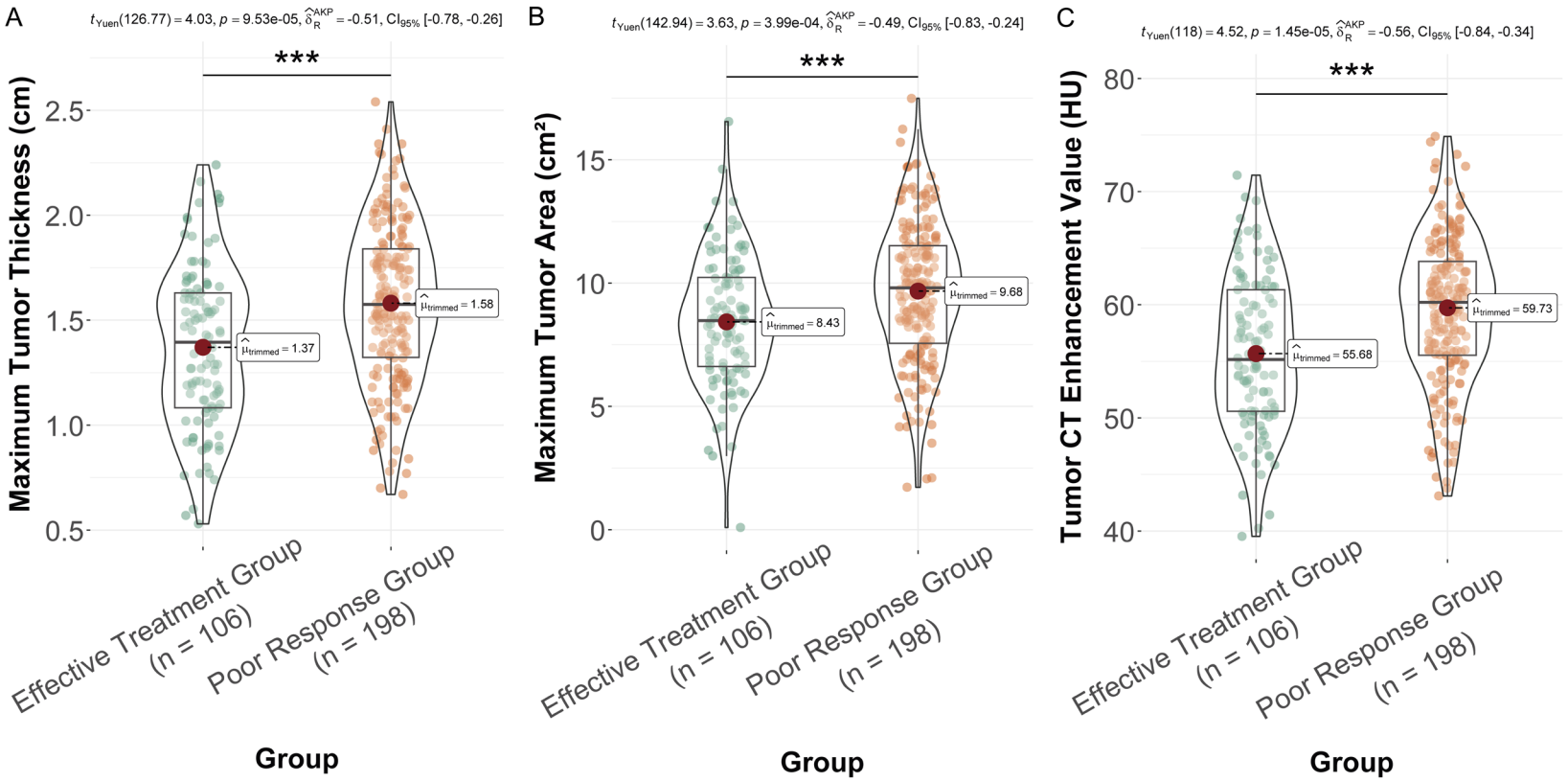

Figure 4. Comparison of quantitative CT imaging parameters at baseline between the two groups in the training set. A. Maximum tumor thickness; B. Maximum tumor area; C. Tumor CT enhancement value. ***P<0.001. Note: CT: Computed Tomography.

Table 3. Univariate correlation analysis of factors affecting poor response to neoadjuvant chemotherapy in the training set

Variable	rho	P
CEA (ng/mL)	0.163	0.004
AFP (ng/mL)	0.178	0.002
CA199 (U/mL)	0.181	0.002
CA724 (U/mL)	0.171	0.003
Tumor Surface Ulceration	0.169	0.003
EMVI Positive	0.149	0.009
Maximum Tumor Thickness (cm)	0.242	<0.001
Maximum Tumor Area (cm^2)	0.203	<0.001
Tumor CT Enhancement Value (HU)	0.249	<0.001

Note: CEA, Carcinoembryonic Antigen; AFP, Alpha-Fetoprotein; CA199, Carbohydrate Antigen 19-9; CA724, Carbohydrate Antigen 72-4; EMVI, Extramural Vascular Invasion; CT, computed tomography.

parameters demonstrated strong associations, with maximum tumor thickness being a particularly potent predictor (OR, 4.931; 95% CI, 2.277-10.678; P<0.001), along with maximum tumor area (OR, 1.225; 95% CI, 1.100-1.356; P<0.001) and tumor CT enhancement value (OR, 1.084; 95% CI, 1.039-1.131; P< 0.001). These results underscore the importance of integrating both serum markers and CT imaging characteristics to predict chemotherapy response more accurately.

Combined predictive mode (training set)

In the training set, a combined predictive model was developed using the random forest algorithm, integrating independent risk factors with predictive value to forecast poor response to neoadjuvant chemotherapy in GEJ adenocarcinoma. The model achieved an area under the curve (AUC) of 0.813. **Figure 5** displays the out-of-bag error rate plot and the variable importance from the random forest. These results suggest that the combined predictive model provides substantial value in predicting poor response to neoadjuvant chemotherapy in GEJ adenocarcinoma.

Performance evaluation and calibration of a predictive nomogram (training set)

To further evaluate the clinical utility of the model, we constructed a nomogram based on multivariate logistic regression and performed detailed calibration and discrimination tests:

Model Calibration: We used calibration curves to assess the agreement between the predicted probabilities from the nomogram and the actual observed frequencies. The calibration curve (**Figure 6**) illustrates the model's performance across different probability thresholds. Ideally, all points should fall on the 45-degree diagonal line, indicating perfect calibration. Our results show that the predicted probabilities from the nomogram align closely with the actual observed frequencies, demonstrating excellent calibration performance.

Discrimination Ability: The discrimination ability of the nomogram was evaluated using the area under the curve (AUC), as shown in **Figure 5**. In the training set, the AUC of the nomogram was 0.813, indicating good discrimination ability. This suggests that the nomogram can effectively distinguish between various response types.

Additionally, **Figure 6** presents the specific structure of the nomogram and its calibration curve, facilitating clinicians in calculating the probability of adverse responses based on individual patient characteristics.

Baseline characteristics (test set)

In the test set analysis, serum markers showed significantly higher levels of CEA, AFP, CA19-9, and CA72-4 in the poor response group compared to the effective treatment group (**Table 5**). Tumor surface ulceration was notably more prevalent in the poor response group, as was EMVI positivity. Quantitative CT parameters also demonstrated significant differences: the poor response group had a greater maximum tumor thickness, a larger maximum tumor area, and higher tumor CT enhancement values. However, demographic factors such as age, BMI, and education level did not significantly differ between groups, nor did qualitative parameters like layered tumor enhancement or vascular and peritoneal invasion. These findings highlight the utility of both serum and imaging markers in predicting chemotherapy response.

Multivariate logistic regression analysis (test set)

The multivariate logistic regression analysis in the test set identified several independent risk

Table 4. Multivariate logistic regression analysis of risk factors for poor response to neoadjuvant chemotherapy in the training set

Risk Factors	Coefficient	Std Error	Wald Stat	P	OR (95% CI)
CEA	0.132	0.062	2.133	0.033	1.141 (1.011-1.288)
AFP	0.114	0.044	2.620	0.009	1.121 (1.029-1.221)
CA199	0.040	0.013	3.001	0.003	1.041 (1.014-1.069)
CA724	0.165	0.053	3.144	0.002	1.180 (1.064-1.308)
Tumor Surface Ulceration	0.893	0.327	2.734	0.006	2.443 (1.288-4.633)
EMVI Positive	0.995	0.433	2.299	0.022	2.704 (1.158-6.314)
Maximum Tumor Thickness	1.595	0.394	4.047	<0.001	4.931 (2.277-10.678)
Maximum Tumor Area	0.203	0.055	3.694	<0.001	1.225 (1.100-1.356)
Tumor CT Enhancement Value	0.081	0.022	3.703	<0.001	1.084 (1.039-1.131)

Note: CEA, Carcinoembryonic Antigen; AFP, Alpha-Fetoprotein; CA199, Carbohydrate Antigen 19-9; CA724, Carbohydrate Antigen 72-4; EMVI, Extramural Vascular Invasion; CT, computed tomography.

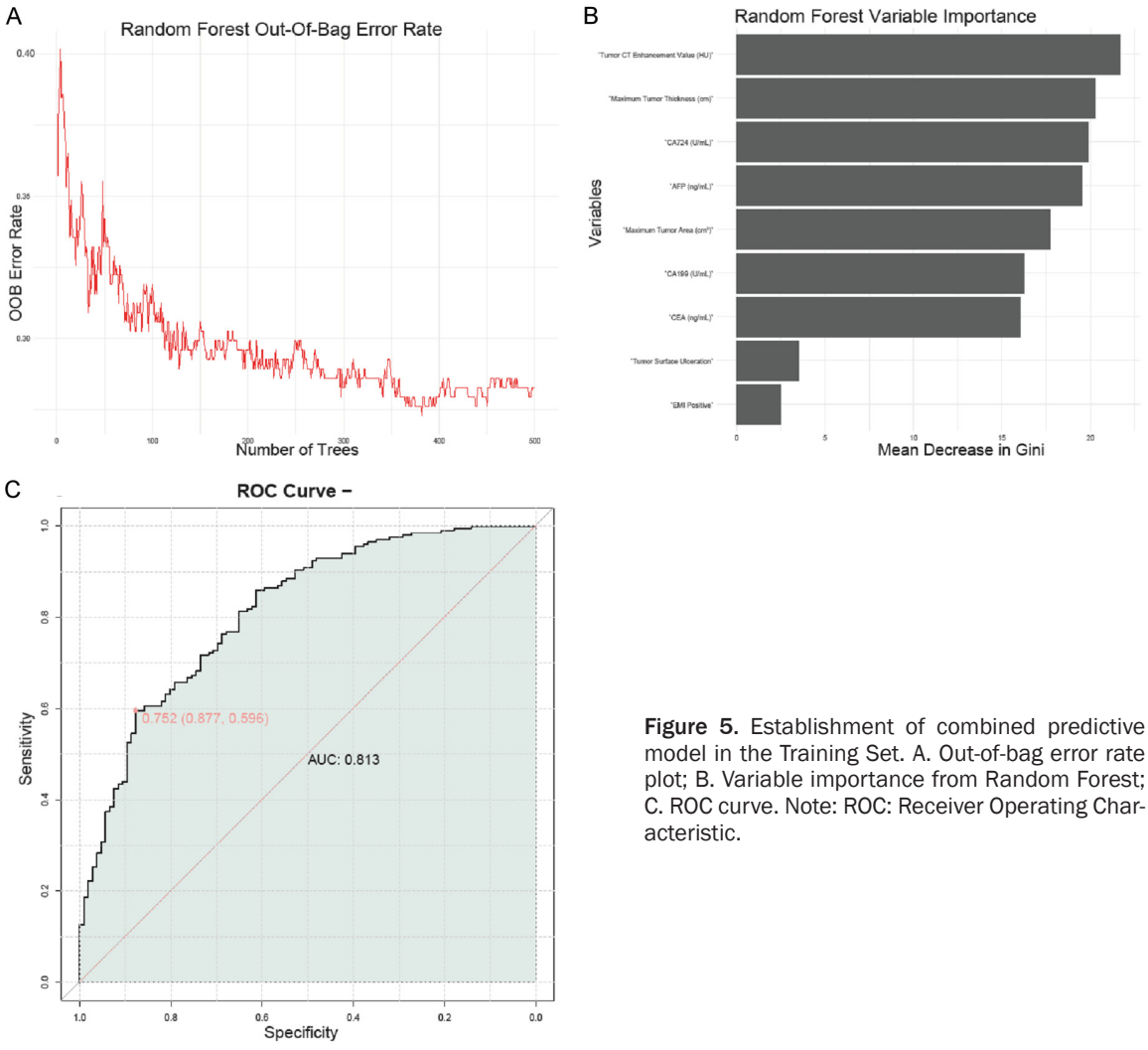

Figure 5. Establishment of combined predictive model in the Training Set. A. Out-of-bag error rate plot; B. Variable importance from Random Forest; C. ROC curve. Note: ROC: Receiver Operating Characteristic.

factors for poor response to neoadjuvant chemotherapy in patients with GEJ adenocarcinoma (**Table 6**). Notably, increased serum levels of CEA were associated with a higher risk, as

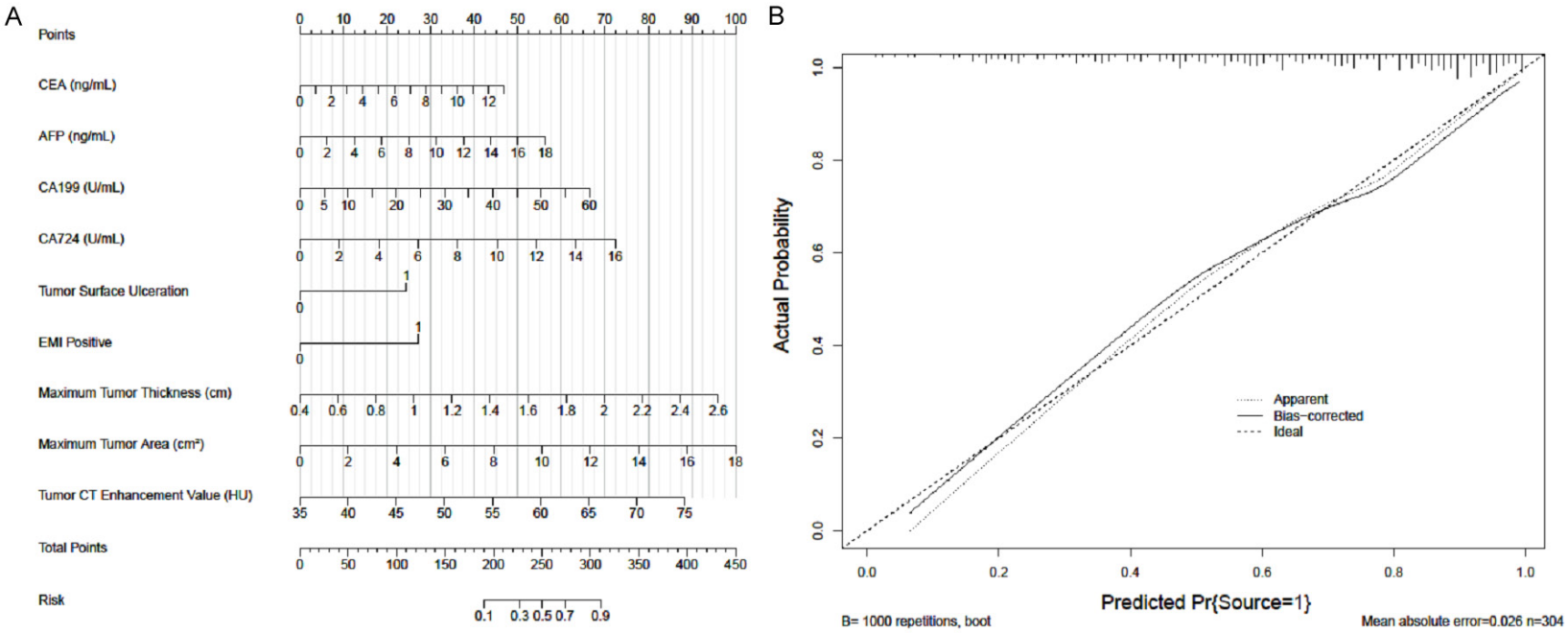

Figure 6. Performance evaluation and calibration of a predictive nomogram. A. Nomogram; B. Calibration curve.

Table 5. Comparison of baseline characteristics between the two groups in the test set

Parameters	Effective Treatment Group (n=93)	Poor Response Group (n=115)	t/χ^2	P
Age (years)	62.43 ± 8.67	63.12 ± 8.39	0.584	0.560
BMI (kg/m^2)	24.18 ± 2.63	23.97 ± 2.54	0.591	0.555
Education Level (years)	12.47 ± 3.22	12.76 ± 3.14	0.657	0.512
Gender [n (%)]			0.064	0.801
Male	64 (68.82%)	81 (70.43%)		
Female	29 (31.18%)	34 (29.57%)		
Employment, work for pay [n (%)]	59 (63.44%)	76 (66.09%)	0.158	0.691
Residential Status [n (%)]			1.394	0.238
Rural	26 (27.96%)	41 (35.65%)		
Urban	67 (72.04%)	74 (64.35%)		
Marital Status [n (%)]			1.504	0.471
Married	78 (83.87%)	96 (83.48%)		
Single	11 (11.83%)	17 (14.78%)		
Divorced	4 (4.30%)	2 (1.74%)		
Smoking history [n (%)]	30 (32.26%)	37 (32.17%)	0	0.99
Drinking history [n (%)]	24 (25.81%)	31 (26.96%)	0.035	0.852
Hypertension [n (%)]	33 (35.48%)	40 (34.78%)	0.011	0.916
Diabetes Mellitus [n (%)]	13 (13.98%)	21 (18.26%)	0.69	0.406
Cardiovascular Disease [n (%)]	10 (10.75%)	17 (14.78%)	0.739	0.39
T Stage [n (%)]			0.122	0.727
T3	54 (57.96%)	64 (55.65%		
T4	39 (41.94%)	51 (44.35%)		
N Stage [n (%)]			2.943	0.4
N0	16 (17.20%)	11 (9.57%)		
N1	26 (27.96%)	37 (32.17%)		
N2	29 (31.18%)	41 (35.65%)		
N3	22 (23.66%)	26 (22.61%)		
Siewert Type [n (%)]			1.05	0.592
Siewert I	2 (2.15%)	1 (0.87%)		
Siewert II	76 (81.72%)	91 (79.13%)		
Siewert III	15 (16.13%)	23 (20.00%)		
CEA (ng/mL)	4.54 ± 2.10	5.41 ± 2.52	2.673	0.008
AFP (ng/mL)	7.27 ± 3.65	8.52 ± 3.11	2.671	0.008
CA199 (U/mL)	28.42 ± 10.74	32.35 ± 11.11	2.57	0.011
CA724 (U/mL)	6.76 ± 2.44	7.72 ± 2.86	2.584	0.01
Tumor Surface Ulceration [n (%)]	21 (22.58%)	47 (40.87%)	7.816	0.005
Layered Enhancement of Tumor [n (%)]	40 (42.98%)	58 (50.43%)	1.137	0.286
Vascular Invasion [n (%)]	18 (19.35%)	32 (27.83%)	2.021	0.155
Peritoneal Invasion [n (%)]	7 (7.53%)	17 (14.78%)	2.652	0.103
EMVI Positive [n (%)]	9 (9.68%)	33 (28.70%)	11.541	<0.001
Maximum Tumor Thickness (cm)	1.36 ± 0.37	1.57 ± 0.37	4.227	<0.001
Maximum Tumor Area (cm^2)	8.45 ± 2.62	9.61 ± 2.86	3.025	0.003
Tumor CT Enhancement Value (HU)	55.74 ± 6.82	59.40 ± 6.48	3.95	<0.001

Note: BMI, body mass index; T Stage, Tumor Stage; N Stage, Node Stage; CEA, Carcinoembryonic Antigen; AFP, Alpha-Fetoprotein; CA199, Carbohydrate Antigen 19-9; CA724, Carbohydrate Antigen 72-4; EMVI, Extramural Vascular Invasion; CT, computed tomography.

Table 6. Multivariate logistic regression analysis of risk factors for poor response to neoadjuvant chemotherapy in the test set

Risk Factors	Coefficient	Std Error	Wald Stat	*P* Value	OR (95% CI)
CEA	0.171	0.080	2.147	0.032	1.187 (1.015-1.388)
AFP	0.130	0.055	2.367	0.018	1.138 (1.023-1.268)
CA199	0.040	0.017	2.359	0.018	1.041 (1.007-1.076)
CA724	0.141	0.067	2.101	0.036	1.152 (1.010-1.314)
Tumor Surface Ulceration	1.112	0.393	2.828	0.005	3.039 (1.407-6.566)
EMVI Positive	1.308	0.478	2.738	0.006	3.699 (1.450-9.433)
Maximum Tumor Thickness	2.216	0.516	4.295	<0.001	9.174 (3.336-25.227)
Maximum Tumor Area	0.238	0.072	3.288	0.001	1.269 (1.101-1.462)
Tumor CT Enhancement Value	0.108	0.029	3.712	<0.001	1.114 (1.052-1.179)

Note: CEA, Carcinoembryonic Antigen; AFP, Alpha-Fetoprotein; CA199, Carbohydrate Antigen 19-9; CA724, Carbohydrate Antigen 72-4; EMVI, Extramural Vascular Invasion; CT, computed tomography.

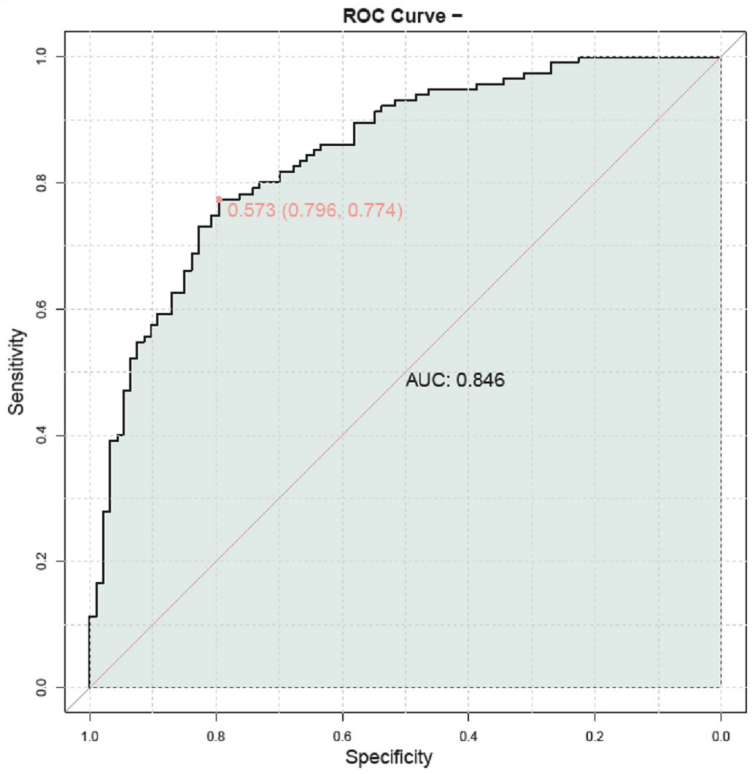

Figure 7. Combined predictive model for assessing risk factors associated with poor response to neoadjuvant chemotherapy in patients with AEG (test cohort). Note: AEG: adenocarcinoma of the esophagogastric junction.

were elevated levels of CA19-9 and CA72-4. Tumor surface ulceration emerged as a significant predictor, increasing the odds of poor response by more than threefold. EMVI positivity further exacerbated this risk. Quantitative imaging features also provided strong indicators, with maximum tumor thickness significantly elevating the risk, alongside maximum tumor area and tumor CT enhancement value. These findings emphasize the predictive strength of integrating serum markers and CT imaging characteristics for assessing chemotherapy response.

Combined predictive mode (test cohort)

In the test set, a combined predictive model was constructed by integrating independent risk factors to forecast poor response to neoadjuvant chemotherapy in GEJ adenocarcinoma. The model demonstrated a high predictive value with an AUC of 0.846 (**Figure 7**). These findings indicate the strong potential of the combined model in predicting adverse reactions to neoadjuvant chemotherapy in this patient population.

Discussion

In this study, we explored the predictive potential of baseline CT imaging features combined with serum biomarkers for forecasting treatment response in patients with adenocarcinoma of the esophagogastric junction (AEG). Our findings underscore the synergistic value of integrating CT imaging characteristics with biological markers, offering a comprehensive approach to predict chemotherapy efficacy [19].

The correlation between CT parameters and chemotherapy response can be understood through tumor biology and therapeutic dynamics. Tumors with greater maximum thickness and area were identified as predictors of poor response, likely due to an increased tumor burden and resistance to therapy [20-22]. These tumors often harbor hypoxic regions, which hinder drug delivery and reduce therapeutic effectiveness. Additionally, larger tumors may exhibit more aggressive cellular phenotypes, posing challenges for neoadjuvant strategies aimed at reducing tumor size before surgery [23, 24].

Higher CT enhancement values indicate increased vascular supply within the tumor, potentially enhancing chemotherapy delivery. However, excessive vascularization might also support rapid tumor growth, indicating the complex role of vascular properties in chemotherapeutic responses [25-27]. The identification of extramural venous invasion (EMVI) as a predictor underscores its detrimental impact on treatment outcomes by facilitating cancer cell dissemination and systemic spread [28, 29].

Our findings regarding serum markers further underscore the interplay between tumor biology and systemic host responses. Elevated levels of CEA, AFP, CA19-9, and CA72-4 were associated with poor chemotherapy response, reflecting their roles in tumor activity and burden. These biomarkers are involved in processes that hinder effective chemotherapy, such as cellular adhesion, immune evasion, metastasis, and oncogenic signaling pathways [30, 31].

The presence of surface ulceration in tumors also correlated with poor response, possibly due to the tumor's underlying biological aggressiveness or altered microenvironment. Ulceration disrupts normal tissue architecture, which may impair local drug penetration and distribution, thereby influencing the pharmacokinetics and local concentrations of chemotherapeutic agents.

This multidimensional approach-integrating both imaging characteristics and serum biomarker analyses-offers a pathway towards more personalized and precise therapeutic planning. The robust discriminative capabilities of our predictive models, validated through rigorous statistical analyses, underscore their potential in clinical settings. Such models could serve as valuable decision-support tools, assisting clinicians in stratifying patients based on predicted chemotherapy responses and tailoring treatment regimens accordingly.

Despite these promising findings, it is crucial to consider potential molecular and genetic alterations that may underlie the observed phenotypic characteristics. Investigating these molecular landscapes could offer additional insights into tumor biology and facilitate the development of targeted therapies complement conventional treatment approaches. Furthermore, identifying and addressing specific risk factors or exploiting tumor microenvironment vulnerabilities may offer new avenues to enhance therapeutic outcomes.

However, several limitations must be acknowledged. The retrospective design of our study may have introduced potential selection bias, limiting generalizability. While we have performed external validation using an independent dataset of 208 patients, the sample size and scope of this dataset still call for future research with larger, more diverse datasets from public databases such as TCGA and GEO. These databases often contain comprehensive clinical, molecular, and genetic data for large cohorts of patients with similar conditions. Integrating these data will help validate and refine our predictive models across different populations and settings.

The current sample size, while sufficient for preliminary assessments, highlights the need for future research with larger, prospective cohorts to further confirm the robustness and generalizability of our findings. Additionally, addressing potential confounding factors, such as genetic mutations and variability in chemotherapy regimens, will be essential for enhancing the applicability of these models in personalized treatment planning. Future studies should also explore advanced machine learning techniques to uncover complex patterns and interactions within the data, thereby improving the predictive accuracy of our models.

Conclusion

In conclusion, the study underscores the predictive value of combining CT imaging characteristics with serum markers for assessing che-

motherapy response in GEJ adenocarcinoma. By elucidating the underlying mechanisms driving these predictions, we can refine our understanding of tumor biology and therapy interactions, ultimately paving the way for more effective and personalized oncological care. As clinical application progresses, integrating these findings into routine practice necessitates ongoing refinement and validation of predictive models, along with broader incorporation of molecular diagnostics to ensure comprehensive patient care and optimized treatment strategies.

Acknowledgements

This study was supported by the Shandong Provincial Medical and Health Science and Technology Development Plan Project (No. 202204010809).

Disclosure of conflict of interest

None.

Address correspondence to: Libo Yu, Department of Imaging, Yantaishan Hospital, No. 10087 Science and Technology Avenue, Laishan District, Yantai 264000, Shandong, China. E-mail: yuliboyantai@163.com

References

[1] Suh YS, Na D, Lee JS, Chae J, Kim E, Jang G, Lee J, Min J, Ock CY, Kong SH, George J, Zhang C, Lee HJ, Kim JI, Kim SJ, Kim WH, Lee C and Yang HK. Comprehensive molecular characterization of adenocarcinoma of the gastroesophageal junction between esophageal and gastric adenocarcinomas. Ann Surg 2022; 275: 706-717.

[2] Huang Q, Cheng Y, Lew E, Shi J, Wiener D and Weber HC. Patients with esophageal adenocarcinoma showed better prognosis than those with adenocarcinoma of the gastroesophageal junction. J Dig Dis 2023; 24: 98-112.

[3] Gamboa A and Naik R. Concise commentary: it's all downhill from here-how diagnostic and therapeutic advances may decrease the incidence rates of gastroesophageal junction and esophageal adenocarcinoma. Dig Dis Sci 2024; 69: 254-255.

[4] Manabe N, Matsueda K and Haruma K. Epidemiological review of gastroesophageal junction adenocarcinoma in asian countries. Digestion 2022; 103: 29-36.

[5] Zandirad E, Teixeira Farinha H, Barberá-Carbonell B, Geinoz S, Demartines N, Schäfer M and Mantziari S. Neoadjuvant chemoradiotherapy versus chemotherapy for gastroesophageal junction adenocarcinoma; which is the optimal treatment option? Cancers (Basel) 2022; 14: 5856.

[6] Li N, Li Z, Fu Q, Zhang B, Zhang J, Wan XB, Lu CM, Wang JB, Deng WY, Ma YJ, Bie LY, Wang MY, Li J, Xia QX, Wei C and Luo SX. Efficacy and safety of neoadjuvant sintilimab in combination with FLOT chemotherapy in patients with HER2-negative locally advanced gastric or gastroesophageal junction adenocarcinoma: an investigator-initiated, single-arm, open-label, phase II study. Int J Surg 2024; 110: 2071-2084.

[7] Verschoor YL, van de Haar J, van den Berg JG, van Sandick JW, Kodach LL, van Dieren JM, Balduzzi S, Grootscholten C, ME IJ, Veenhof A, Hartemink KJ, Vollebergh MA, Jurdi A, Sharma S, Spickard E, Owers EC, Bartels-Rutten A, den Hartog P, de Miranda N, van Leerdam ME, Haanen J, Schumacher TN, Voest EE and Chalabi M. Neoadjuvant atezolizumab plus chemotherapy in gastric and gastroesophageal junction adenocarcinoma: the phase 2 PANDA trial. Nat Med 2024; 30: 519-530.

[8] Ferreira JE, Mbagwu E, Lee EY, Shelman NR and Allison DB. Cytopathological features of gastroesophageal junction adenocarcinoma with enteroblastic differentiation and histopathological correlation. Cytopathology 2023; 34: 250-253.

[9] Mahuron KM, Sullivan KM, Hernandez MC, Chen YJ, Chao J, Melstrom LG, Paz IB, Kim JY, Mannan R, Lin JL, Fong Y and Woo Y. Diffuse-type histology is prognostic for all siewert types of gastroesophageal adenocarcinoma. J Gastric Cancer 2024; 24: 267-279.

[10] Wu M, Sheng M, Li R, Zhang X, Chen X, Liu Y, Liu B, Yu Y and Li X. Dual-layer dual-energy CT for improving differential diagnosis of squamous cell carcinoma from adenocarcinoma at gastroesophageal junction. Front Oncol 2022; 12: 979349.

[11] Li KY, Ou J, Zhou HY, Yu ZY, Gao D, You XY, Zhang XM, Li R and Chen TW. Gross tumor volume of adenocarcinoma of esophagogastric junction corresponding to cT and cN stages measured with computed tomography to quantitatively determine resectabiliy: a case control study. Front Oncol 2022; 12: 1038135.

[12] Owens C, Hindocha S, Lee R, Millard T and Sharma B. The lung cancers: staging and response, CT, (18)F-FDG PET/CT, MRI, DWI: review and new perspectives. Br J Radiol 2023; 96: 20220339.

[13] Hien PN, Chun HJ, Oh JS, Kim SH and Choi BG. Usefulness of tumor perfusion on cone-beam CT after hepatic arterial infusion port implantation for evaluating tumor response to hepat-

ic arterial infusion chemotherapy in hepatocellular carcinoma treatment. Diagn Interv Radiol 2023; 29: 832-837.
[14] Pang G, Shao C, Lv Y and Zhao F. Tumor attenuation and quantitative analysis of perfusion parameters derived from tri-phasic CT scans in hepatocellular carcinoma: relationship with histological grade. Medicine (Baltimore) 2021; 100: e25627.
[15] Shibata C, Nakano T, Yasumoto A, Mitamura A, Sawada K, Ogawa H, Miura T, Ise I, Takami K, Yamamoto K and Katayose Y. Comparison of CEA and CA19-9 as a predictive factor for recurrence after curative gastrectomy in gastric cancer. BMC Surg 2022; 22: 213.
[16] Dislich B, Kröll D and Langer R. Surgical pathology of adenocarcinomas arising around or within the gastroesophageal junction. Updates Surg 2023; 75: 395-402.
[17] Chen HY, Feng LL, Li M, Ju HQ, Ding Y, Lan M, Song SM, Han WD, Yu L, Wei MB, Pang XL, He F, Liu S, Zheng J, Ma Y, Lin CY, Lan P, Huang MJ, Zou YF, Yang ZL, Wang T, Lang JY, Orangio GR, Poylin V, Ajani JA, Wang WH and Wan XB. College of American pathologists tumor regression grading system for long-term outcome in patients with locally advanced rectal cancer. Oncologist 2021; 26: e780-e793.
[18] Huang W, Li L, Liu S, Chen Y, Liu C, Han Y, Wang F, Zhan P, Zhao H, Li J and Gao J. Enhanced CT-based radiomics predicts pathological complete response after neoadjuvant chemotherapy for advanced adenocarcinoma of the esophagogastric junction: a two-center study. Insights Imaging 2022; 13: 134.
[19] Lauk O, Patella M, Neuer T, Battilana B, Frauenfelder T, Nguyen-Kim TDL, Weder W, Caviezel C, Hillinger S, Inci I and Opitz I. Implementing CT tumor volume and CT pleural thickness into future staging systems for malignant pleural mesothelioma. Cancer Imaging 2021; 21: 48.
[20] Wongwaiyut K, Ruangsin S, Laohawiriyakamol S, Leelakiatpaiboon S, Sangthawan D, Sunpaweravong P and Sunpaweravong S. Pretreatment esophageal wall thickness associated with response to chemoradiotherapy in locally advanced esophageal cancer. J Gastrointest Cancer 2020; 51: 947-951.
[21] Je HJ, Cho SH, Oh HS, Seo AN, Park BG, Lee SM, Kim SH, Kim GC, Ryeom H and Choi GS. Response prediction after neoadjuvant chemotherapy for colon cancer using CT tumor regression grade: a preliminary study. J Korean Soc Radiol 2023; 84: 1094-1109.
[22] Wang ZL, Li YL, Li XT, Tang L, Li ZY and Sun YS. Role of CT in the prediction of pathological complete response in gastric cancer after neoadjuvant chemotherapy. Abdom Radiol (NY) 2021; 46: 3011-3018.
[23] Travis WD, Dacic S, Wistuba I, Sholl L, Adusumilli P, Bubendorf L, Bunn P, Cascone T, Chaft J, Chen G, Chou TY, Cooper W, Erasmus JJ, Ferreira CG, Goo JM, Heymach J, Hirsch FR, Horinouchi H, Kerr K, Kris M, Jain D, Kim YT, Lopez-Rios F, Lu S, Mitsudomi T, Moreira A, Motoi N, Nicholson AG, Oliveira R, Papotti M, Pastorino U, Paz-Ares L, Pelosi G, Poleri C, Provencio M, Roden AC, Scagliotti G, Swisher SG, Thunnissen E, Tsao MS, Vansteenkiste J, Weder W and Yatabe Y. IASLC multidisciplinary recommendations for pathologic assessment of lung cancer resection specimens after neoadjuvant therapy. J Thorac Oncol 2020; 15: 709-740.
[24] Saw SPL, Ong BH, Chua KLM, Takano A and Tan DSW. Revisiting neoadjuvant therapy in non-small-cell lung cancer. Lancet Oncol 2021; 22: e501-e516.
[25] Esteves M, Monteiro MP and Duarte JA. The effects of vascularization on tumor development: a systematic review and meta-analysis of preclinical studies. Crit Rev Oncol Hematol 2021; 159: 103245.
[26] De Palma M and Hanahan D. Milestones in tumor vascularization and its therapeutic targeting. Nat Cancer 2024; 5: 827-843.
[27] Zheng R, Li F, Li F and Gong A. Targeting tumor vascularization: promising strategies for vascular normalization. J Cancer Res Clin Oncol 2021; 147: 2489-2505.
[28] Bates DDB, Homsi ME, Chang KJ, Lalwani N, Horvat N and Sheedy SP. MRI for rectal cancer: staging, mrCRM, EMVI, lymph node staging and post-treatment response. Clin Colorectal Cancer 2022; 21: 10-18.
[29] Lord AC, D'Souza N, Shaw A, Rokan Z, Moran B, Abulafi M, Rasheed S, Chandramohan A, Corr A, Chau I and Brown G. MRI-diagnosed tumor deposits and EMVI status have superior prognostic accuracy to current clinical TNM staging in rectal cancer. Ann Surg 2022; 276: 334-344.
[30] Force M, Park G, Chalikonda D, Roth C, Cohen M, Halegoua-DeMarzio D and Hann HW. Alpha-fetoprotein (AFP) and AFP-L3 is most useful in detection of recurrence of hepatocellular carcinoma in patients after tumor ablation and with low AFP level. Viruses 2022; 14: 775.
[31] Egbert L, Norain A, Stucky CC, Ahmad S, Chang YH and Wasif N. Cancer embryonic antigen (CEA) levels in patients with appendiceal adenocarcinoma predict response to neo-adjuvant chemotherapy and overall survival. J Surg Oncol 2023; 127: 688-698.